Title

Inlet and outlet valve flow and regurgitant volume may be directly and reliably quantified with accelerated, volumetric phase-contrast MRI

Journal

Journal of Magnetic Resonance Imaging, 41(2)

ISSN

1053-1807

Authors

Hsiao, Albert
Tariq, Umar
Alley, Marcus T
et al.

Publication Date

2015-02-01

DOI

10.1002/jmri.24578

Peer reviewed

Published in final edited form as:
J Magn Reson Imaging. 2015 February ; 41(2): 376–385. doi:10.1002/jmri.24578.

Inlet and outlet valve flow and regurgitant volume may be directly and reliably quantified with accelerated, volumetric phase-contrast MRI

Albert Hsiao, MD, PhD[1], **Umar Tariq, MBBS**[1], **Marcus T. Alley, PhD**[1], **Michael Lustig, PhD**[2], and **Shreyas S. Vasanawala, MD, PhD**[1]

[1]Department of Radiology, Stanford University

[2]Department of Electrical Engineering and Computer Science, University of California, Berkeley

Abstract

Purpose—To determine whether it is feasible to use solely an accelerated 4D-PC MRI acquisition to quantify net and regurgitant flow volume through each of the cardiac valves.

Materials and Methods—Accelerated, 4D-PC MRI examinations performed between March 2010 through June 2011 as part of routine MRI examinations for congenital, structural heart disease were retrospectively reviewed and analyzed using valve-tracking visualization and quantification algorithms developed in Java and OpenGL. Excluding patients with transposition or single ventricle physiology, a total of 34 consecutive pediatric patients (19 male, 15 female; mean age 6.9 years; age range 10 months-15 years) were identified. 4D-PC flow measurements were compared at each valve and against routine measurements from conventional cardiac MRI using Bland-Altman and Pearson correlation analysis.

Results—Inlet and outlet valve net flow were highly correlated between all valves (ρ=0.940–0.985). The sum of forward flow at the outlet valve and regurgitant flow at the inlet valve were consistent with volumetric displacements each ventricle (ρ=0.939–0.948). These were also highly consistent with conventional planar MRI measurements of with net flow (ρ=0.923–0.935) and regurgitant fractions (ρ=0.917–0.972) at the outlet valve and ventricular volumes (ρ=0.925–0.965).

Conclusion—It is possible to obtain consistent measurements of net and regurgitant blood flow across the inlet and outlet valves relying solely on accelerated 4D-PC. This may facilitate more efficient clinical quantification of valvular regurgitation.

Keywords

flow; structural; tricuspid; mitral; regurgitation

Albert Hsiao, Department of Radiology, Stanford University, 300 Pasteur Drive S-072, Stanford, CA 94305, alhsiao@stanford.edu, ph: (858) 335-2173, fax: (888) 872-8162, Shreyas S. Vasanawala, MD, PhD, Department of Radiology, Stanford University, 725 Welch Rd., Rm 1679 MC 5913, Stanford, CA 94305-5654, vasanawala@stanford.edu, ph: (650) 724-9824, fax: (650) 723-8402.

Disclosures:
AH and SSV are consultants for Morpheus Medical.

INTRODUCTION

Chronic inlet valve regurgitation, tricuspid or mitral, results in chronic volume loading of the corresponding ventricle and when sufficiently severe, and can contribute to ventricular failure[1]. It is for this reason that imaging follow-up is increasingly utilized to follow patients with chronic valvular insufficiency to assess the optimal timing of surgical intervention. This is particularly the case in chronic mitral insufficiency, in light of recommendations for earlier repair[2]. Inlet valve regurgitation is however difficult to reliably quantify by current imaging modalities, whether by directly interrogating the regurgitant jet or by indirectly assessing the regurgitant orifice or ventricular displacements[3]. This challenge is due, in part, to the dynamic nature of the inlet valves, which translate substantially during the cardiac cycle as the cardiac chambers contract around them.

While quantitative MRI is a well-validated clinical technique and is generally felt to be a reliable methodology for quantification of blood flow[4–6] and ventricular volumes[7], particularly for the right heart. It has been shown to have lower interobserver variability for measuring volume of regurgitation at the aortic valve than TTE[7]. For the inlet valves however, reliable assessment of volume of regurgitation is challenging. Conventional planar phase-contrast imaging (2D-PC) of the inlet valve is typically prescribed as a static plane, and because of the translation of the valve plane, is generally not simultaneously reliable for quantification of forward flow and regurgitant volume. Correlations between flow through the inlet and outlet valves have been only moderate using the 2D approach[8,9]. Furthermore, precise positioning and orientation of this plane requires both technical expertise and an understanding of structural heart disease at the time of image acquisition, which can pose significant problems to managing clinical workflow in a busy imaging practice. Because of these limitations, some have even argued to perform a focused TTE of the inlet valve at the time of the MRI to better assess inlet valve regurgitation[10].

Volumetric phase-contrast MRI, also known as 4D phase-contrast (4D-PC) MRI, is an evolving technique that overcomes some of the current limitations of cardiac MRI[9,11–14]. During a single acquisition, cine anatomic data and a vector field of velocity data are acquired simultaneously. This enables retrospective evaluation of blood flow, without the need for precise scan prescription at the time of image-acquisition[15]. Several studies have now shown that it is possible to quantify blood flow using 4D-PC with comparable or even improved accuracy and precision relative to conventional planar phase-contrast MRI[15–18], particularly at the aortic and pulmonary valves. In addition, recent advances in accelerated imaging have made it feasible to acquire a volume of millimeter-resolution data across the entire chest in roughly 10 minutes[16,19]. These highly-accelerated, high signal-to-noise acquisitions have made it possible to directly visualize the function of each of the valves using velocity-fusion volume-rendering[19]. We hypothesized that it may also be possible to use solely an accelerated 4D-PC MRI acquisition to quantify net and regurgitant flow through each of the valves.

MATERIALS AND METHODS

Subjects

With institutional review board approval and HIPAA compliance, we retrospectively identified patients for whom a compressed-sensing 4D-PC acquisition of the chest was performed as part of a routine clinical MRI examination from March of 2010 through June of 2011. Informed consent for off-label MRI acquisitions were obtained prior to each exam. 49 examinations were identified. Patients with single-ventricle physiology were excluded, since for the remaining subjects the left and right heart cardiac outputs can serve as an internal control. Patients with transposition of the great arteries were also excluded to simplify comparison of inlet and outlet valve flows with ventricular displacements of each ventricle. A total of 15 examinations were excluded, leaving 34 examinations in the study (19 male, 15 female; mean age 6.9 years; age range 10 months-15 years). No additional selection or exclusion criteria were used. Demographics are provided in table 1.

Conventional MRI

All MR imaging was performed on a 1.5-T TwinSpeed MRI scanner with an eight-channel phased array cardiac coil (GE Healthcare, Milwaukee, WI), 150 T/ms maximum slew rate, 40 mT/min gradients, and vector ECG gating. For the conventional portion of the exam, imaging acquisition planes were prescribed by one of three board-certified radiologists with dedicated cardiovascular training and 5 (SSV), 7, and greater than 10 years of experience in pediatric cardiovascular MRI. MRI examinations were tailored to the clinical indication and typically included multiple 8–10 mm thick 2D-PC scan planes at the outflow valves and at any additional sites of interest noted at the time of image acquisition. These were acquired with a GRE sequence (FastCard, GE Healthcare) with 4–10 views per segment depending on patient heart rate. Parallel-imaging was not employed. 20 cardiac phases were reconstructed. SSFP cine MR images were acquired as axial, short-axis cine, left and right 2- and 3-chamber, and 4-chamber views with slice thickness of 6–8 mm, depending on patient size, with a flip angle of 45°. For these latter views, single signal average breath-held acquisitions were used in patients capable of breath-holding. Otherwise, 2–3 signal-average free-breathing acquisitions were used to reduce respiratory artifact. Total scan times ranged from 25 minutes to 1 hour and 37 minutes (mean 55 minutes), depending on clinical indication and scan protocol, excluding the 4D-PC acquisition. Quantitative analysis of 2D-PC and SSFP data was performed with QFlow (version 5.2, MEDIS) and QMass software (version 7.2, MEDIS), respectively. In order to account for background phase-error, a region of interest in static soft tissue near the vessel of interest was used to estimate local background phase-error. This background phase-error was then subtracted from the flow measurement.

4D-PC scans

Each 4D-PC acquisition was performed following contrast-enhanced MRA performed with off-label intravenous administration of gadofosveset to provide enhanced signal-to-noise and support higher acceleration. 4D-PC MRI was performed using a SPGR-based sequence with tetrahedral flow-encoding and variable-density Poisson-disc k-space undersampling[20,21] with total acceleration factors ranging from 1.6×1.6 to 2.2×2.2, covering the entire chest

with phase-encoding in the anterior-posterior direction. Zero-filling interpolation (ZIP) of 2 was applied in the slice direction. Images were reconstructed for each cardiac temporal phase separately with a combined autocalibrating parallel imaging compressed sensing algorithm (L_1-SPIRiT)[22]. Compressed-sensing was implemented to take advantage of per-slice 2D spatial sparsity without enforcing temporal sparsity. K-space phase-reordering was employed for respiratory compensation (EXORCIST, GE Healthcare, Milwaukee, WI). No respiratory gating was used. No signal averaging (NEX) was employed. A flip angle of 15° and 2–4 tetrahedral encodes per segment were used. Velocity-encoding parameters were selected to avoid velocity aliasing, ranging from 150–300 cm/s, based on clinical indication for the examination and presence of aliasing on conventional 2D phase-contrast MRI planes. True spatial resolution, accounting for zero-filling interpolation averaged 1.04 × 1.38 × 2.41-mm, ranging from 0.78–1.41-mm in the RL-direction, 1.04–1.88-mm in the AP-direction, and 2.00–3.40-mm in the SI-direction. Mean TR and TE were 4.8 ms and 1.8 ms, respectively. Temporal resolutions ranged from 33–86 ms (mean 61 ms). 20 cardiac phases were reconstructed. Acquisition times ranged from 7 to 15 minutes (mean 10 minutes, 10 seconds). Image reconstructions were performed with a GPGPU implementation of L_1-SPIRIT[23] on a 64-bit Linux workstation equipped with four Tesla C1060 graphics cards (NVIDIA, Santa Clara, CA). Image data were corrected for Maxwell phase effects[24], encoding errors related to gradient field distortions[25], and eddy-current related phase offsets[16,26].

4D-PC quantitation

A quantitative 4D-PC analysis approach was developed and implemented in Java (version 1.6.0, Oracle) and OpenGL (version 1.1, SGI), building upon a visualization and quantification framework previously described[15,16,19]. Four viewing planes were provided, one primary cross-sectional view and three additional cross-reference windows. Functionality was provided to manually translate and rotate these cross-reference windows into two-chamber, three-chamber, and four-chamber views of either ventricle (figure 1, supplemental video 1). To enable inlet-valve valve-tracking, software controls were created allow placement and adjustment of a temporally-resolved cross-sectional plane and manual contouring of the valve annulus at any temporal phase. For ventricular volume quantification, a panel of 24 short axis views through each ventricle was provided, marked with the position of the valve plane and apex. Segmentations of the left and right ventricle were performed from these views at end-systole and end-diastole in a manner previously described[16].

For each of the outlet valves, a static cross-sectional plane was defined orthogonal to early systolic blood flow. For each of the inlet valves, an initial valve plane was centered at the valve, oriented orthogonal to early diastolic flow. If needed, this plane was manually rotated into the plane of the valve annulus, approximately along the atrioventricular groove. The location of the cross-sectional plane was adjusted at end-diastole and end-systole. End-diastole was defined as the last phase prior to forward flow through the outlet valve, while end-systole was defined as the last phase prior to forward flow through the inlet valve. The position of the plane for temporal phases in-between were interpolated from user-specified locations. If the dynamic plane did not adequately match the valve plane at any temporal

phase, the plane was adjusted and phases in-between were automatically interpolated. Segmentations of the valve plane were created at the same key temporal phases and automatically interpolated in-between. For the mitral valve, careful attention was made to exclude blood flow through the left ventricular outflow tract. Cross-sectional area, maximal valve displacement, net blood flow and regurgitant fraction measurements were each tabulated.

All valve tracking planes and segmentations were supervised by a board-certified radiologist with four years of experience in segmentation of congenital cardiac MRI (AH). Measurements at each valve were performed in triplicate by a research assistant with 1 year of experience with cardiac MRI (UT). Segmentations were obtained at and near the valve plane, approximately 1-mm apart. Using an approach previously described for volumetric segmentation of 4D anatomic data[16], left and right ventricular volumes were separately segmented at end-diastole and end-systole from 4D-PC images. Upon completion of all segmentations, quantitative ventricular volumes and blood flow measurements were calculated at each valve (figure 2, supplemental figure 1). Total post-processing time for 4D-PC was approximately 60 minutes – evenly divided between valvular flow quantification and ventricular volumetry.

Statistical Analyses

Statistical analyses were performed with custom macros defined in Excel 2007 (Microsoft, Redmond, WA). First, we assessed the consistency of net blood flow measurements between each of the valves among patients without intracardiac or extracardiac shunts. For all study patients, we identified patients with shunts by reviewing prior TTE reports and the 4D-PC study[19]. In patients without shunts, net blood flow rates at all valves are expected to be identical to satisfy conservation of mass. Aortic, pulmonary, mitral, and tricuspid blood flows were compared with each other using Pearson correlation and Bland-Altman analysis. Bland-Altman limits of agreement were calculated and reported as 1.96 times the standard deviation of the difference of measurements.

Second, we compared phase-contrast blood flow measurements at the valves to volumetric displacements between end-diastole and end-systole of the corresponding ventricle. We defined displaced ventricular blood volume (ΔV) for the each ventricle by: $\Delta V = (V_{ED} - V_{ES}) \times HR$, where V_{ED} was the end-diastolic volume, V_{ES} was the end-systolic volume, and HR was the patient's heart rate. This displaced blood volume should exceed the net flow at the inlet or outlet valve by exactly the amount of regurgitant blood flow at both of these valves. For this, we computed the estimated displaced blood volume (ΔV_{est}) computed from 4D phase-contrast blood flow measurements according to:

$$\Delta V_{est} = Q_{OV} + Q_{OV}\frac{RF_{OV}}{1 - RF_{OV}} + Q_{IV}\frac{RF_{IV}}{1 - RF_{IV}},$$

where Q_{OV} was the measured net blood flow at the outlet valve, Q_{IV} was the measured net blood flow at the inlet valve, RF_{OV} was the measured regurgitant fraction at the outlet valve and RF_{IV} was the measured regurgitant fraction at the inlet valve. The displaced volumes were compared using Pearson correlation and Bland-Altman analysis.

Lastly, for all patients included in the study, we compared blood flow and volumetric measurements obtained from 4D-PC data to routinely obtained blood flow measurements using 2D-PC and volumetric measurements using SSFP imaging. These were compared using Pearson correlation and Bland-Altman analysis.

RESULTS

Valvular anatomy

The mean cross-sectional area of the mitral valve annulus during diastole was 4.8 cm^2 (range 2.2–9.2 cm^2). Tricuspid valves measured slightly larger, with a mean 7.0 cm^2 (range 3.0–12.3 cm^2). As anticipated, the inlet valves each had considerable displacement over the course of the cardiac cycle. Between end-diastole and end-systole, the mitral valve had a mean excursion distance of 11.4 mm (range 5.4–17.2 mm). The tricuspid valve had a similar excursion distance, averaging 11.8 mm (range 6.3–19.3 mm).

Consistency of net flow through different valves

In patients without intracardiac or extracardiac shunts (*n*=26), 4D phase-contrast blood flow measurements were tightly correlated at each of the valves (table 2, figure 3). In our study, flow rates were most tightly matched between the aortic and pulmonary valves (ρ=0.985). Though still tightly correlated, the weakest correlation was found between the mitral and tricuspid valves (ρ=0.936). Limits of agreement between transvalvular flow measurements were narrow (18–32%), comparable to prior studies comparing free-breathing and breath-held flow measurements of the ascending aorta and main pulmonary artery by conventional phase-contrast[27]. Mitral and tricuspid valve measurements slightly underestimated net flow relative to their outlet valves aortic valve by 0.184 L/min (6%) and 0.091 L/min (3%), respectively. There was only one case in which the mitral flow exceeded aortic flow, which was explained by a shunt from the left ventricle through the coronary sinus into the left atrium in a patient with prior repair of an atrioventricular canal defect.

Consistency between displaced volumes and transvalvular flow

In patients without shunts, we further validated the accuracy of flow measurements by comparing them against blood volume displaced by the left and right ventricles (table 2, figure 4). In the absence of intracardiac shunting, the displaced blood volume, calculated from the difference in ventricular volume at end-diastole and end-systole, should exactly match the net flow at the outlet valve plus the regurgitant flow at the inlet and outlet valves. For both the left and right heart, there was tight correlation (ρ=0.939, 0.948) between ventricular displacements computed by either method with no significant bias (4%, 3%) and narrow B-A limits of agreement (29%, 23%).

Comparison between 4D-PC and conventional MRI

To assess the consistency of flow measurements against more established quantitative techniques, we additionally compared 4D-PC against conventional 2D phase-contrast MRI. 2D phase-contrast flow measurements were obtained in 27 of the 34 patients. In these comparisons, there was good correlation between 4D-PC and 2D-PC measurements of aortic and pulmonary blood flow (ρ=0.935, 0.934). In our hands, blood flow measured slightly

greater by 2D-PC than by 4D-PC with B-A mean differences of 0.48 and 0.19 L/min (17% and 14%) at the aortic and pulmonary valves respectively (figure 5), which was statistically significant (paired *t-test*, $\rho<0.05$). This was consistent with a prior study that showed 2D-PC flow measurements typically exceeded displacements of ventricular volume, even in patients without valvular insufficiency[16]. Regurgitant fractions at the aortic and pulmonary valves nevertheless correlated well between 4D-PC and 2D-PC ($\rho=0.972$, 0.933) with no significant bias and narrow agreement (13% and 14%).

Lastly, we compared ventricular volumes obtained from 4D-PC against conventional SSFP (table 3, figure 5). SSFP volumetry of the left and right ventricle was performed in 27 of the 34 clinical MRI studies. Volumetric measurements of the left and right ventricle were strongly correlated between the two methodologies ($\rho=0.925$, 0.965). There was no significant bias (2%, −3%) in ventricular volumes and limits of agreement were narrow (29%, 33%).

DISCUSSION

We demonstrate here that with a single accelerated 4D-PC MRI acquisition of the chest, it is possible to accurately quantify inlet and outlet valve flow and regurgitation volume. Although inlet valve flow and regurgitant volume quantification can be technically challenging for current imaging modalities, we have shown that with dynamic valve-tracking visualization, it is possible to obtain quantitative measurements across all four valves solely from this acquisition. These flow measurements are consistent between valves, consistent with volumetric assessments of ventricular blood displacement, and consistent with the proven clinical reference standards of valvular blood flow and ventricular volume, namely conventional 2D-PC and SSFP imaging. The high degree of data redundancy and internal consistency provided by this imaging approach provides new opportunities to assure that the quantitative data provided by cardiac MRI can be reliably reproduced.

Although planar phase-contrast MRI has until now been the standard for non-invasive measurement of blood flow, its current implementation is not without flaws. Several groups have now called upon MRI vendors to better optimize acquisition strategies and equipment to reduce the influence of several factors known to impair the accuracy of 2D-PC[28,29]. In particular, eddy-current-related phase-errors continue to negatively impact accuracy of phase-contrast blood flow measurement. While these phase-errors can also impact 4D-PC, there is more static soft-tissue data available to support computational methods for phase-error correction. We suspect that the slight systematic difference between 2D-PC and 4D-PC blood flow measurements at our institution may be due in part to more accurate phase-error correction in our implementation of 4D-PC.

In our experience, the excursion of the inlet valves is often so wide that any static plane invariably captures portions of the atrium during some phases and portions of the ventricle at others. This has been a long-standing limitation of conventional planar phase-contrast MRI. Earlier works has shown that valve-tracking may be performed for 4D-PC using SSFP imaging planes to follow the location of the valve[8,9]. While these pioneering works demonstrated that such measurements were possible using 4D-PC, these former approaches

required a set of SSFP imaging planes to serve as an anatomic reference to plan a focused field-of-view acquisition on the inlet valve. We present here a novel method of approaching valve-tracking that is solely reliant on a comprehensive whole chest 4D-PC acquisition in the hope that such a method could one day obviate the need for conventional MR imaging planes in select patients.

While echocardiography has been the predominant and most widely available method for functional assessment of the heart[2], it may not by itself be universally sufficient for diagnosis and surgical planning. There are a number of circumstances when it may be difficult to determine based on TTE alone whether surgical intervention is necessary. Sonographic windows may limit visualization, and MRI may be called upon to better evaluate valvular blood flow. Even when the quality of TTE imaging is felt to be adequate, the interpretation and grading of valvular pathology has been shown to be widely variable, even among experienced readers[30]. This can be problematic in the management of both patients with inlet valvular insufficiency in whom valve replacement surgery may be driven primarily on imaging findings[31]. A quantitative metric based on 4D-PC MRI may be more reproducible and could be helpful for developing more systematic evidence-based guidelines for surgical intervention. Since TTE will likely remain much more widely accessible than MRI, future studies should be directed at correlating echocardiographic findings of inlet regurgitation with the method of regurgitant volume quantification presented here.

Until recently, 4D-PC has primarily been of research interest, and flavors of this pulse sequence have been evolving in multiple variations over the last twenty years. While 4D-PC is now routinely acquired at our institution in patients who undergo MRA as part of their clinical congenital cardiac MRI, there are several issues that will need to be resolved to bring this sequence into routine practice. One open question is how to prospectively select the optimal velocity-encoding speed for 4D-PC. In this study, 4D-PC was preceded by conventional 2D-PC imaging planes, which were helpful for identifying the minimal encoding speed needed to avoid velocity-wrapping. In a recent study however, it was shown that venous blood flow could be reliably quantified at arterial encoding speeds when 4D-PC was acquired with intravenous gadofosveset on board[32]. This suggests that selection of a high velocity-encoding speed (i.e. 250 cm/s) may be effective for the majority of studies, though variable-encoding speed approaches may have incremental benefit. As 4D-PC makes its way more commonly into clinical practice, future studies may be needed to determine what velocity-encoding speeds optimal for each clinical indication. For example, in our clinical practice, we anticipate higher velocity-encoding speeds for assessment of pulmonary stenosis and insufficiency, while lower velocity-encoding speeds are more optimal for the assessment of Fontan circulation.

We have routinely used a blood-pool contrast agent, gadofosveset, ahead of the 4D-PC acquisition to improve signal-to-noise and facilitate highly accelerated acquisitions. It is possible that the use of this agent may also have improved velocity-to-noise so that precise velocity-encoding speed selection was not necessary. One limitation of the current study is that we have not thoroughly examined the necessity of contrast administration for the accuracy of flow quantification. In an earlier study, we showed that the precision of aortic and pulmonary flow measurements of 4D-PC was superior to 2D-PC after conventional

gadolinium contrast MRA at more modest spatial resolution and at lower acceleration factors[15]. It is possible that similar results might be obtained without intravenous contrast, but future studies may need to be performed to determine the range of acceleration factors that can be used in a non-contrast setting, while preserving adequate image quality for diagnostic interpretation.

In conclusion, simultaneous measurement of ventricular function and blood flow at all four valves using a single accelerated 4D-PC acquisition has potential to address a significant need, while addressing a current clinical dilemma. It is a challenge in most clinical MRI practices, particularly those with a congenital heart disease focus, to accomplish routinely a quantitative cardiac examination within an hour. It has been our experience that such exams require careful on-site supervision by an experienced cardiac imager to obtain adequate imaging data. In such examinations, measurements of inlet valve flow are often inconsistent with other calculations, due in part to the technical challenge of performing these measurements with available planar acquisitions. If a 4D-PC acquisition can be performed without such oversight, and software is adequately engineered to optimize the use of physician time in interpreting the data, it may become feasible to perform routine quantitative analysis of cardiac function by MRI, whenever echocardiography is felt to be insufficient. Such an exam could serve a significant clinical need, while maximizing the effectiveness of MRI and physician time.

Supplementary Material

Refer to Web version on PubMed Central for supplementary material.

Acknowledgements

Special thanks to Dr. Frandics Chan and Dr. Beverley Newman for mentorship and support of this work.

Funding Sources:

The authors wish to thank the Tashia and John Morgridge Faculty Scholar Fund for generously supporting this work. We would also like to acknowledge grant support from the Lucas Foundation, NIH R01 EB009690 (SSV, MTA, ML), NIH P41 EB015891 (MTA), research support from General Electric (SSV, MTA), UC Discovery Grant #193037 (ML), American Heart Association Grant #12BGIA9660006 (ML) and graphics workstations from NVIDIA (AH, SSV).

REFERENCES

1. Geva T. Repaired tetralogy of Fallot: the roles of cardiovascular magnetic resonance in evaluating pathophysiology and for pulmonary valve replacement decision support. J. Cardiovasc. Magn. Reson. 2011; 13:9. [PubMed: 21251297]
2. Bonow RO, Carabello Ba, Chatterjee K, de Leon AC, Faxon DP, Freed MD, Gaasch WH, Lytle BW, Nishimura Ra, O'Gara PT, O'Rourke Ra, Otto CM, Shah PM, Shanewise JS, Smith SC, Jacobs AK, Adams CD, Anderson JL, Antman EM, Fuster V, Halperin JL, Hiratzka LF, Hunt Sa, Lytle BW, Nishimura R, Page RL, Riegel B. ACC/AHA 2006 guidelines for the management of patients with valvular heart disease: a report of the American College of Cardiology/American Heart Association Task Force on Practice Guidelines (writing Committee to Revise the 1998 guidelines for the manage. J. Am. Coll. Cardiol. 2006; 48:e1–e148. [PubMed: 16875962]
3. Thavendiranathan P, Phelan D, Thomas JD, Flamm SD, Marwick TH. Quantitative assessment of mitral regurgitation: validation of new methods. J. Am. Coll. Cardiol. 2012; 60:1470–1483. [PubMed: 23058312]

4. Higgins CB, Sakuma H. Heart disease: functional evaluation with MR imaging. Radiology. 1996; 199:307–315. [PubMed: 8668769]

5. Szolar DH, Sakuma H, Higgins CB. Cardiovascular applications of magnetic resonance flow and velocity measurements. J Magn Reson Imaging. 1996; 6:78–89. [PubMed: 8851410]

6. Pelc NJ, Herfkens RJ, Shimakawa A, Enzmann DR. Phase contrast cine magnetic resonance imaging. Magn Reson Q. 1991; 7:229–254. [PubMed: 1790111]

7. Cawley PJ, Hamilton-Craig C, Owens DS, Krieger EV, Strugnell WE, Mitsumori L, D'Jang CL, Schwaegler RG, Nguyen KQ, Nguyen B, Maki JH, Otto CM. Prospective comparison of valve regurgitation quantitation by cardiac magnetic resonance imaging and transthoracic echocardiography. Circ. Cardiovasc. Imaging. 2013; 6:48–57. [PubMed: 23212272]

8. Van der Hulst AE, Westenberg JJ, Kroft LJ, Bax JJ, Blom NA, de Roos A, Roest AA. Tetralogy of fallot: 3D velocity-encoded MR imaging for evaluation of right ventricular valve flow and diastolic function in patients after correction. Radiology. 2010; 256:724–734. [PubMed: 20634432]

9. Westenberg JJM, Roes SD, Ajmone Marsan N, Binnendijk NMJ, Doornbos J, Bax JJ, Reiber JHC, de Roos A, van der Geest RJ. Mitral valve and tricuspid valve blood flow: accurate quantification with 3D velocity-encoded MR imaging with retrospective valve tracking. Radiology. 2008; 249:792–800. [PubMed: 18849503]

10. Geva T. Indications and timing of pulmonary valve replacement after tetralogy of Fallot repair. Semin. Thorac. Cardiovasc. Surg. Pediatr. Card. Surg. Annu. 2006; l:11–22. [PubMed: 16638542]

11. Bley TA, Johnson KM, Francois CJ, Reeder SB, Schiebler ML, B RL, Consigny D, Grist TM, Wieben O. Noninvasive assessment of transstenotic pressure gradients in porcine renal artery stenoses by using vastly undersampled phase-contrast MR angiography. Radiology. 2011; 261:266–273. [PubMed: 21813739]

12. Bogren HG, Buonocore MH. 4D magnetic resonance velocity mapping of blood flow patterns in the aorta in young vs. elderly normal subjects. J Magn Reson Imaging. 1999; 10:861–869. [PubMed: 10548800]

13. Markl M, Draney MT, Hope MDMD, Levin JMMD, Chan FPMDPHD, Alley MTPHD, Pelc NJSCD, Herfkens RJMD. Time-Resolved 3-Dimensional Velocity Mapping in the Thoracic Aorta: Visualization of 3-Directional Blood Flow Patterns in Healthy Volunteers and Patients. J. Comput. Assist. Tomogr. July/August. 2004; 28:459–468.

14. Hope MD, Hope TA, Meadows AK, Ordovas KG, Urbania TH, Alley MT, Higgins CB. Bicuspid aortic valve: four-dimensional MR evaluation of ascending aortic systolic flow patterns. Radiology. 255:53–61. [PubMed: 20308444]

15. Hsiao A, Alley MT, Massaband P, Herfkens RJ, Chan FP, Vasanawala SS. Improved cardiovascular flow quantification with time-resolved volumetric phase-contrast MRI. Pediatr. Radiol. 2011; 41:711–720. [PubMed: 21221566]

16. Hsiao A, Lustig M, Alley MT, Murphy M, Chan FP, Herfkens RJ, Vasanawala SS. Rapid pediatric cardiac assessment of flow and ventricular volume with compressed sensing parallel imaging volumetric cine phase-contrast MRI. AJR. Am. J. Roentgenol. 2012; 198:W250–W259. [PubMed: 22358022]

17. Roes SD, Hammer S, van der Geest RJ, Marsan NA, Bax JJ, Lamb HJ, Reiber JH, de Roos A, Westenberg JJ. Flow Assessment Through Four Heart Valves Simultaneously Using 3-Dimensional 3-Directional Velocity-Encoded Magnetic Resonance Imaging With Retrospective Valve Tracking in Healthy Volunteers and Patients With Valvular Regurgitation. Invest Radiol. 2009

18. Brix L, Ringgaard S, Rasmusson A, Sorensen TS, Kim WY. Three dimensional three component whole heart cardiovascular magnetic resonance velocity mapping: comparison of flow measurements from 3D and 2D acquisitions. J Cardiovasc Magn Reson. 2009; 11:3. [PubMed: 19232119]

19. Hsiao A, Lustig M, Alley MT, Murphy MJ, Vasanawala SS. Evaluation of Valvular Insufficiency and Shunts with Parallel-imaging Compressed-sensing 4D Phase-contrast MR Imaging with Stereoscopic 3D Velocity-fusion Volume-rendered Visualization. Radiology. 2012; 265:87–95. [PubMed: 22923717]

20. Vasanawala SS, Murphy MJ, Alley MT, Lai P, Keutzer K, Pauly JM, Lustig M. Practical parallel imaging compressed sensing MRI: Summary of two years of experience in accelerating body MRI of pediatric patients. Proc. IEEE Int. Symp. Biol. Imaging 2011. 2011:1039–1043.
21. Vasanawala SS, Alley MT, Hargreaves BA, Barth RA, Pauly JM, Lustig M. Improved Pediatric MR Imaging with Compressed Sensing. Radiology. 2010; 256:607–616. [PubMed: 20529991]
22. Lustig M, Pauly JM. SPIRiT: Iterative self-consistent parallel imaging reconstruction from arbitrary k-space. Magn. Reson. Med. 2010; 64:457–471. [PubMed: 20665790]
23. Murphy M, Alley MT, Demmel J, Keutzer K, Vasanawala SS, Lustig M. Fast L1-SPIRiT Compressed Sensing Parallel Imaging MRI: Scalable Parallel Implementation and Clinically Feasible Runtime. IEEE Tras Med Imag.
24. Bernstein MA, Zhou XJ, Polzin JA, King KF, Ganin A, Pelc NJ, Glover GH. Concomitant gradient terms in phase contrast MR: analysis and correction. Magn Reson Med. 1998; 39:300–308. [PubMed: 9469714]
25. Markl M, Bammer R, Alley MT, Elkins CJ, Draney MT, Barnett A, Moseley ME, Glover GH, Pelc NJ. Generalized reconstruction of phase contrast MRI: analysis and correction of the effect of gradient field distortions. Magn Reson Med. 2003; 50:791–801. [PubMed: 14523966]
26. Walker PG, Cranney GB, Scheidegger MB, Waseleski G, Pohost GM, Yoganathan AP. Semiautomated method for noise reduction and background phase error correction in MR phase velocity data. J. Magn. Reson. Imaging. 1993; 3:521–530. [PubMed: 8324312]
27. Steeden JA, Atkinson D, Hansen MS, Taylor AM, Muthurangu V. Rapid flow assessment of congenital heart disease with high-spatiotemporal-resolution gated spiral phase-contrast MR imaging. Radiology. 2011; 260:79–87. [PubMed: 21415248]
28. Kilner PJ, Gatehouse PD, Firmin DN. Flow measurement by magnetic resonance: a unique asset worth optimising. J Cardiovasc Magn Reson. 2007; 9:723–728. [PubMed: 17613655]
29. Gatehouse PD, Rolf MP, Graves MJ, Hofman MB, Totman J, Werner B, Quest RA, Liu Y, von Spiczak J, Dieringer M, Firmin DN, van Rossum A, Lombardi M, Schwitter J, Schulz- Menger J, Kilner PJ. Flow measurement by cardiovascular magnetic resonance: a multicentre multi-vendor study of background phase offset errors that can compromise the accuracy of derived regurgitant or shunt flow measurements. J Cardiovasc Magn Reson. 2010; 12:5. [PubMed: 20074359]
30. Biner S, Rafique A, Rafii F, Tolstrup K, Noorani O, Shiota T, Gurudevan S, Siegel RJ. Reproducibility of proximal isovelocity surface area, vena contracta, and regurgitant jet area for assessment of mitral regurgitation severity. JACC. Cardiovasc. Imaging. 2010; 3:235–243. [PubMed: 20223419]
31. Grayburn PA, Bhella P. Grading severity of mitral regurgitation by echocardiography: science or art? JACC. Cardiovasc. Imaging. 2010; 3:244–246. [PubMed: 20223420]
32. Tariq U, Hsiao A, Alley M, Zhang T, Lustig M, Vasanawala SS. Venous and arterial flow quantification are equally accurate and precise with parallel imaging compressed sensing 4D phase contrast MRI. J. Magn. Reson. Imaging. 2012; 37:1419–1426. [PubMed: 23172846]

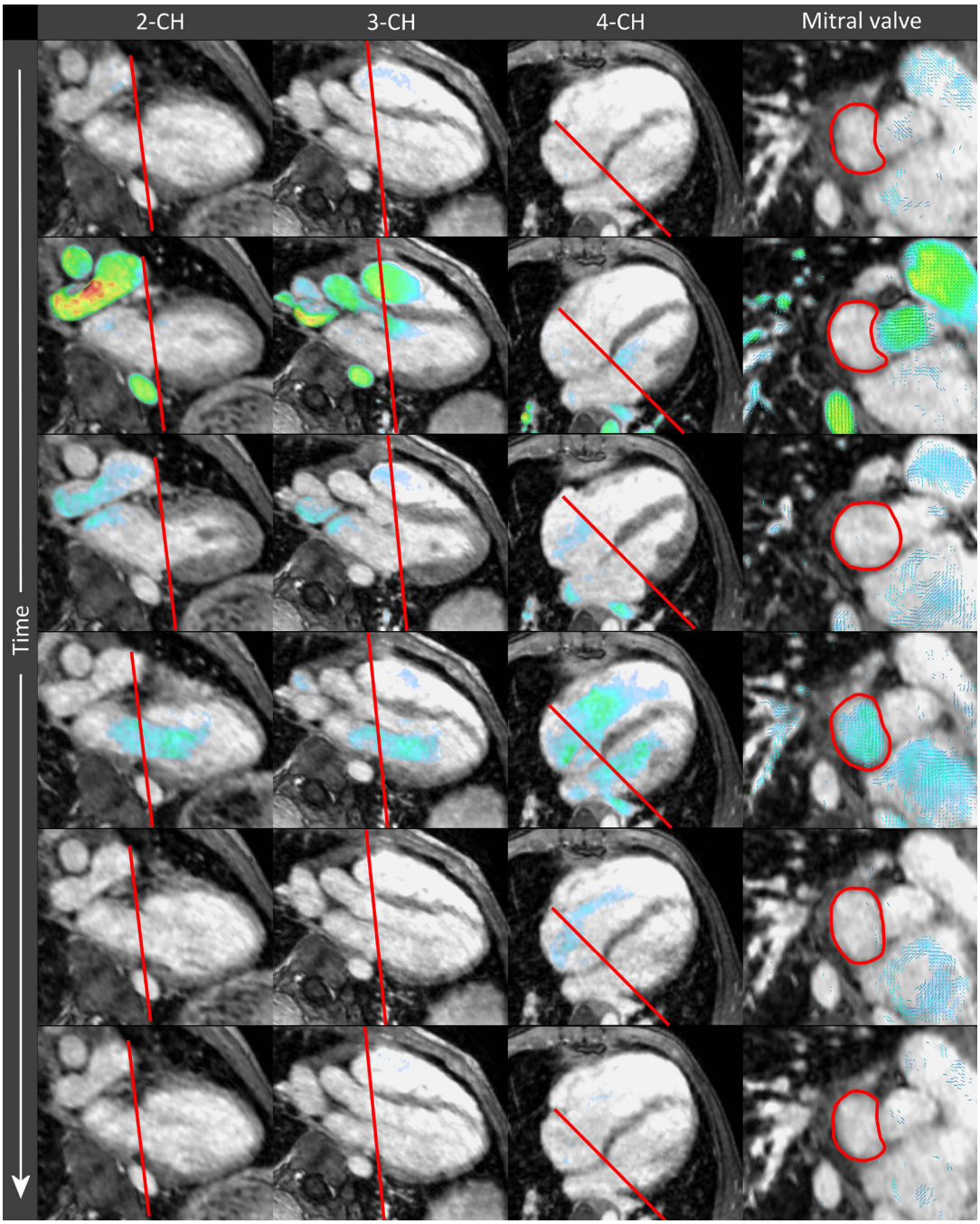

Figure 1.

Inlet-valve tracking (red line) is enabled by simultaneous flow and anatomic visualization, time-resolved definition of the inlet valve plane, and segmentation of the valve annulus. Using a combination of views, including the left ventricular two-chamber, three-chamber and four-chamber views, the inlet-valve plane can be oriented so that the boundaries of the annulus can be manually segmented (right-most column) at each phase of the cardiac cycle.

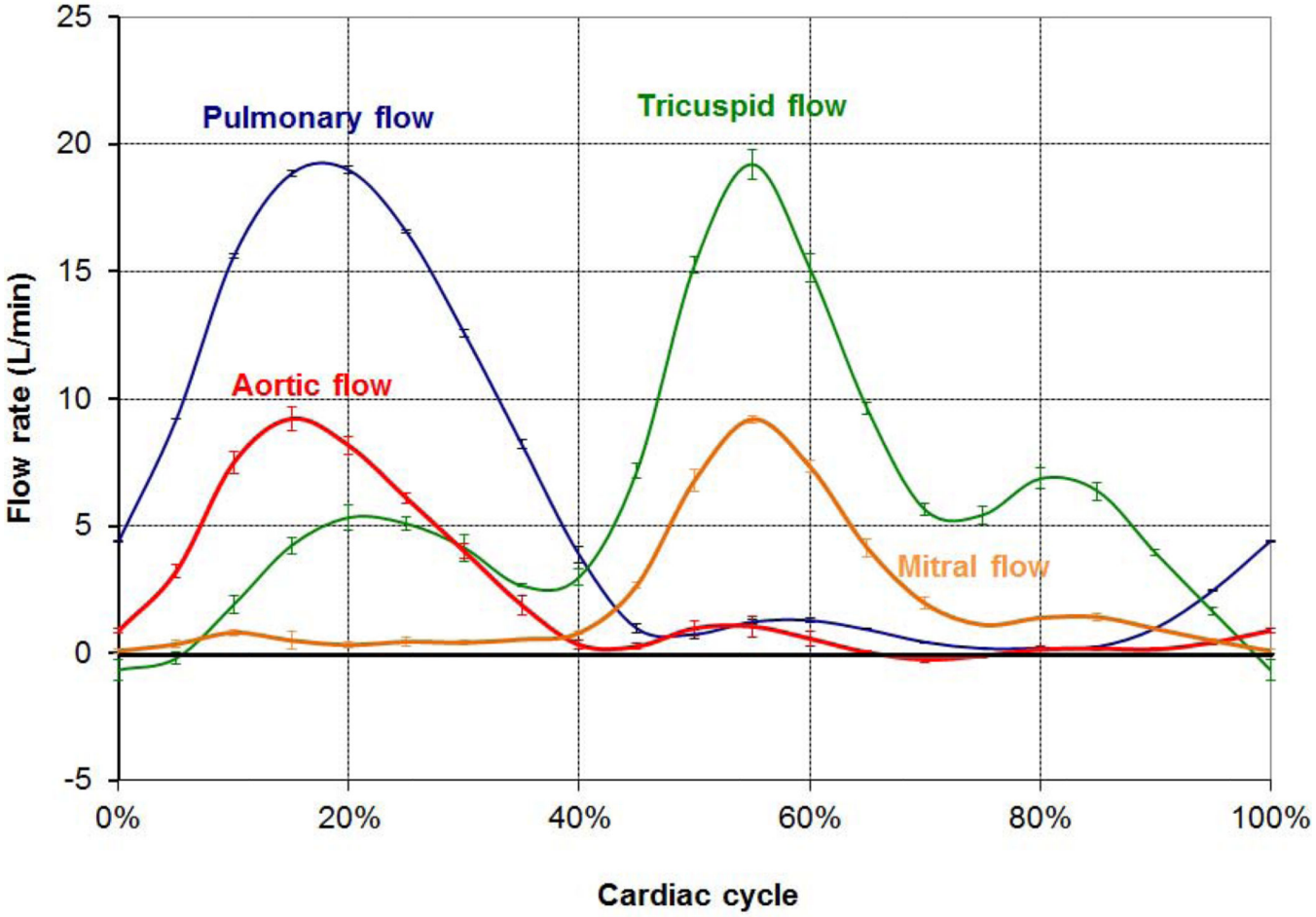

Figure 2.

Representative measurement of valvular blood flow at all four valves in a 6 year old boy with partial anomalous pulmonary venous return. The right-to-left shunt results in increased net blood flow across the tricuspid and pulmonary valves. Error bars display the standard deviation between replicate measurements at each time point.

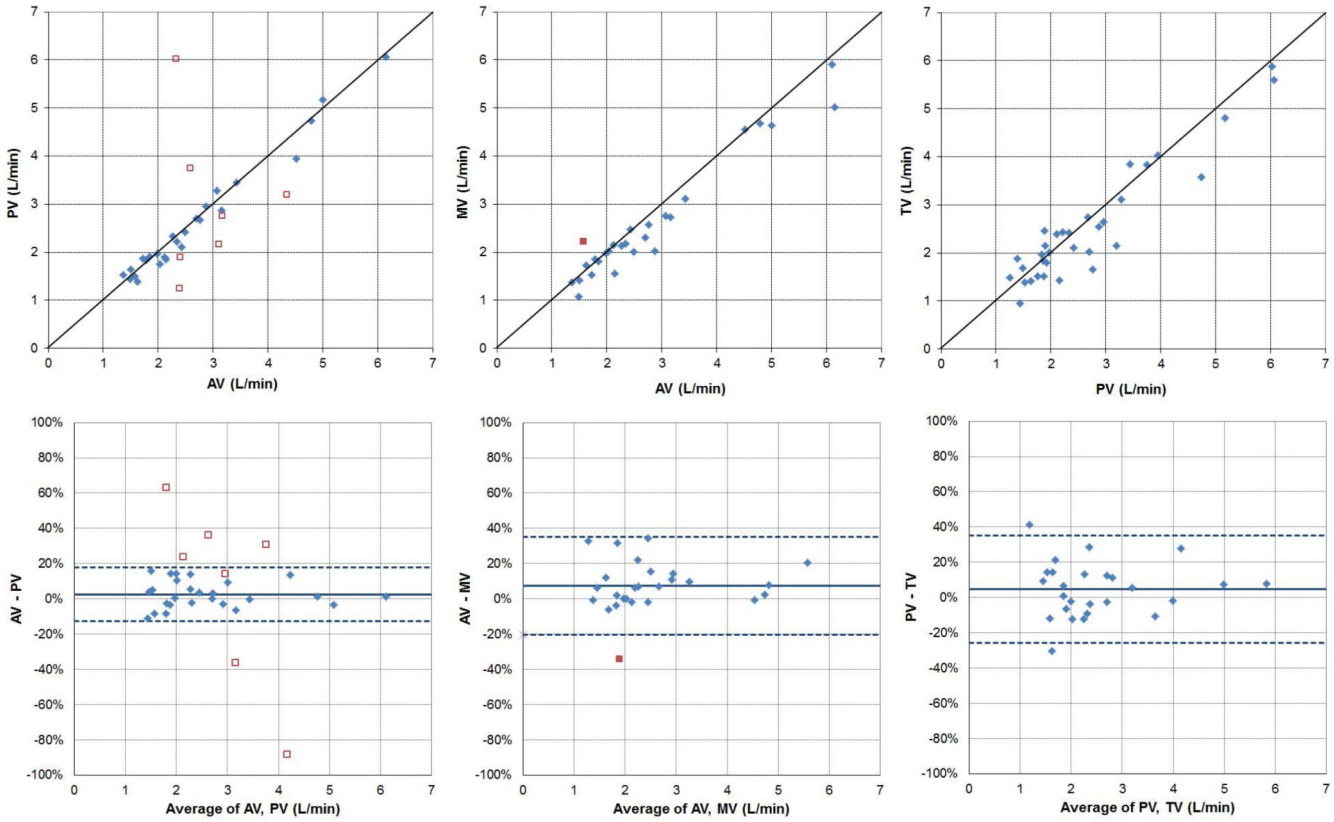

Figure 3.

Correlation of net inlet and outlet blood flow measurements displayed as scatter plots (top row) and Bland-Altman diagrams (bottom row). Dashed lines show the limits of agreement (± 1.96 SD). In (a), aortic and pulmonary valve flow measurements correlated tightly among patients without shunts (blue diamonds). Patients with visually detectable shunts by TTE or 4D-PC are also displayed, clearly distant from the line of identity (red open squares). In (b), aortic and mitral valve blood flow measurements were strongly correlated, though mitral valve flow was slightly underestimated. The single patient with a shunt through the coronary sinus is shown (red closed square). In (c), pulmonary and tricuspid valve flow measurements were well-correlated.

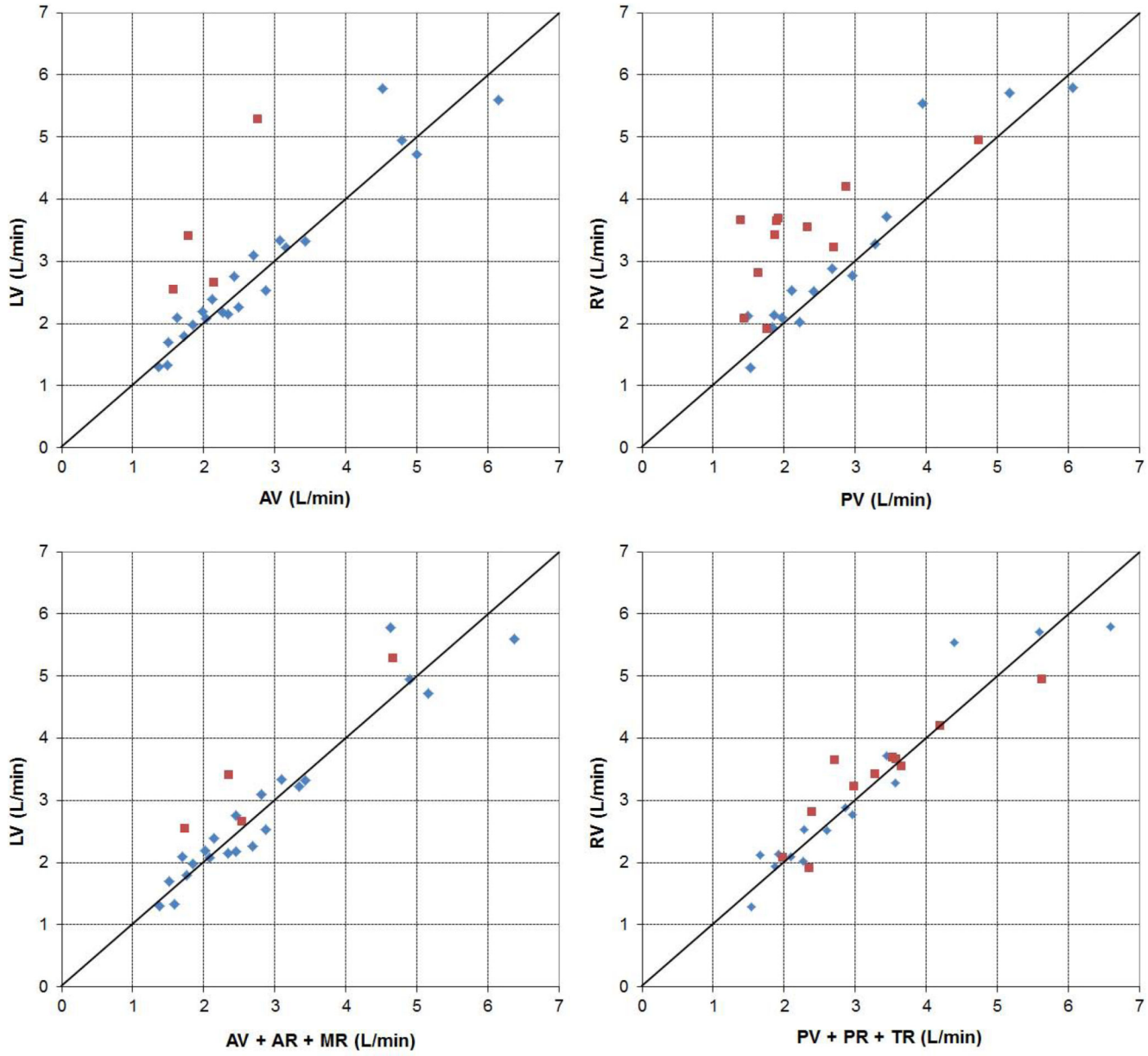

Figure 4.

Correlation between ventricular volume displacement and valvular blood flow before (top-row) and after (bottom-row) accounting for regurgitant flow. Ventricles with greater than 10% regurgitant fraction at either the inlet or outlet valve are shown in red squares. The remaining ventricles are shown in blue diamonds. For both the left ventricle (left) and right ventricle (right), measurements of cardiac output based on ventricular volumes closely matched blood flow measurements only after regurgitant blood flow was accounted for (bottom-row).

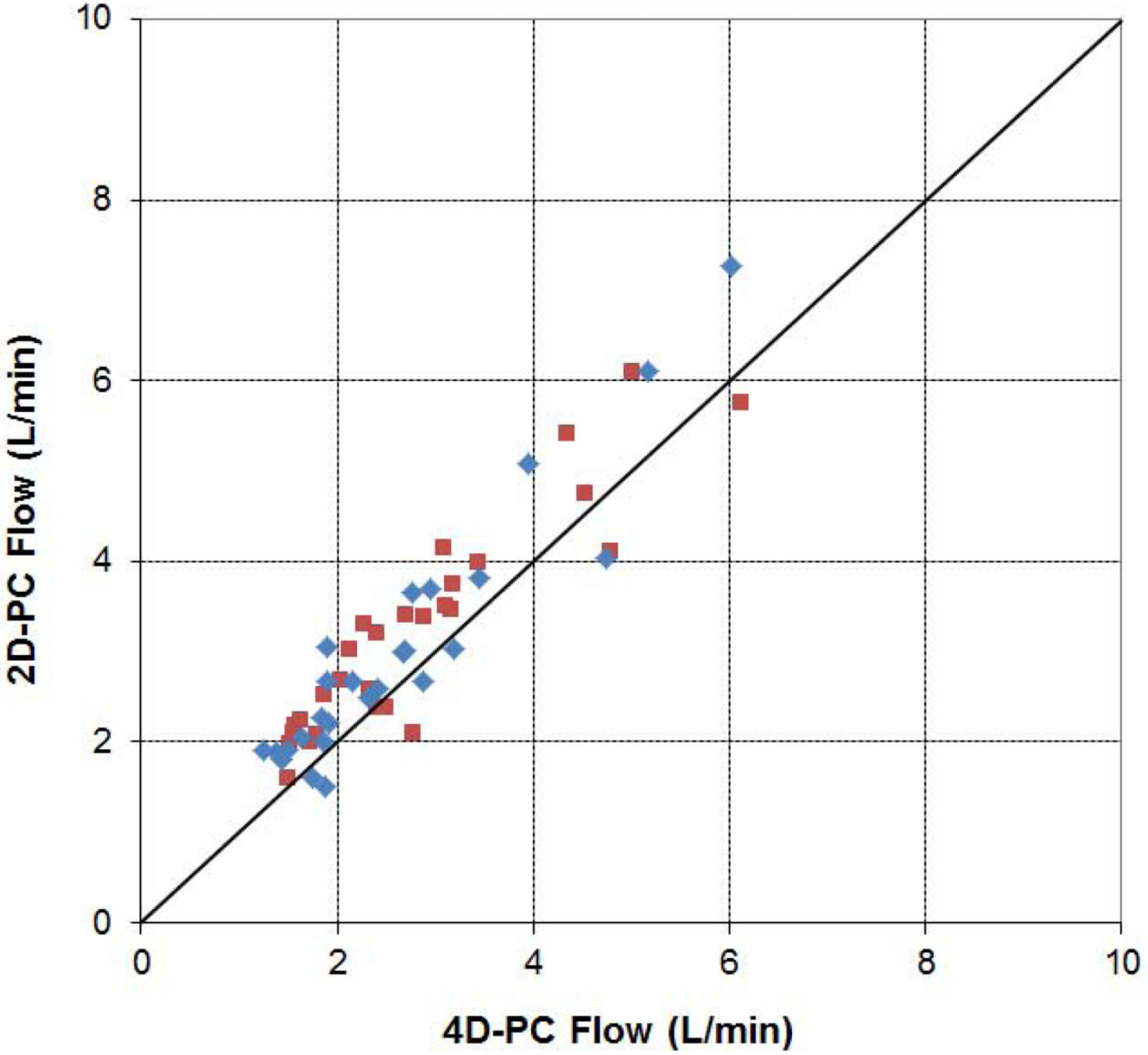

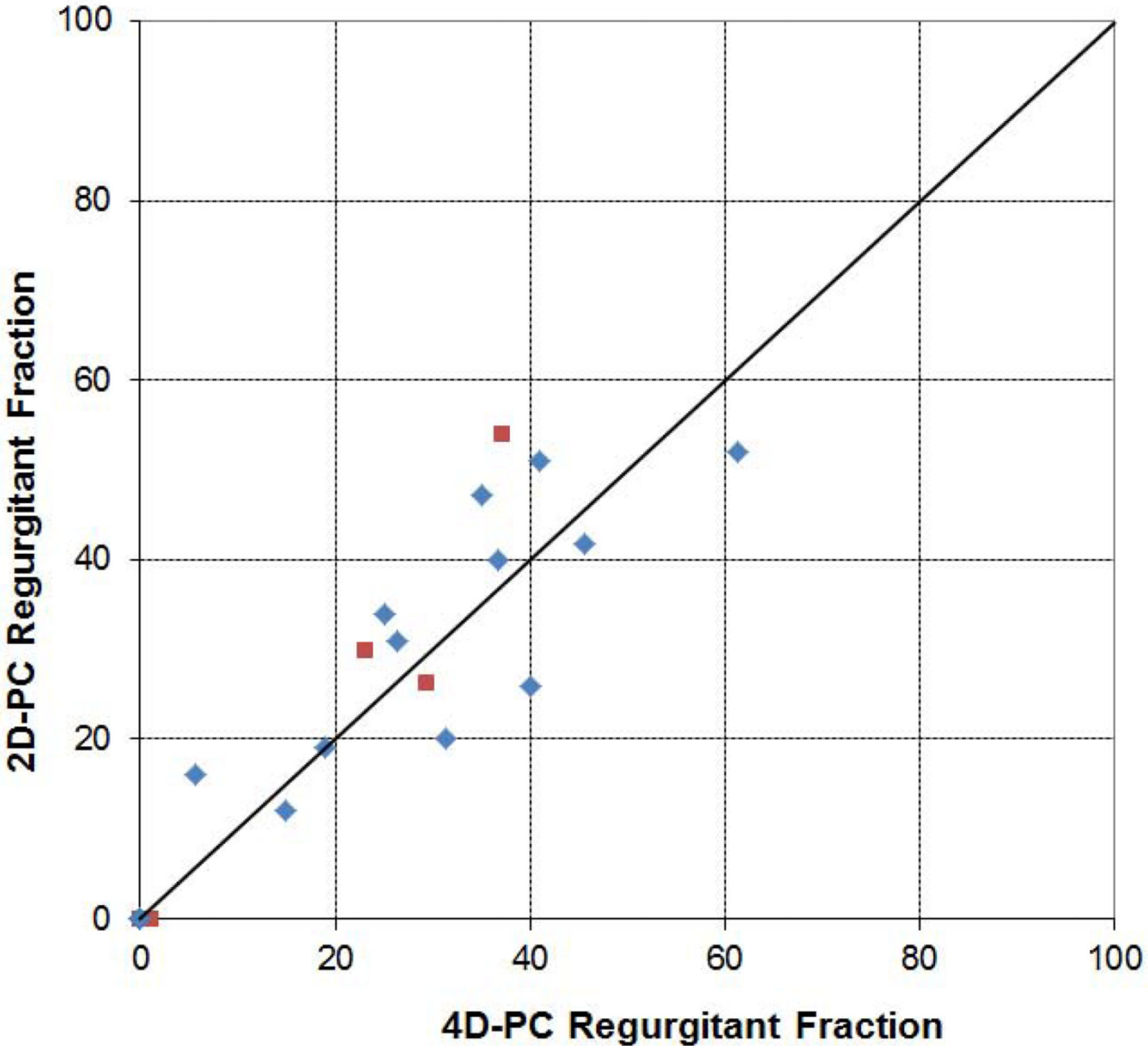

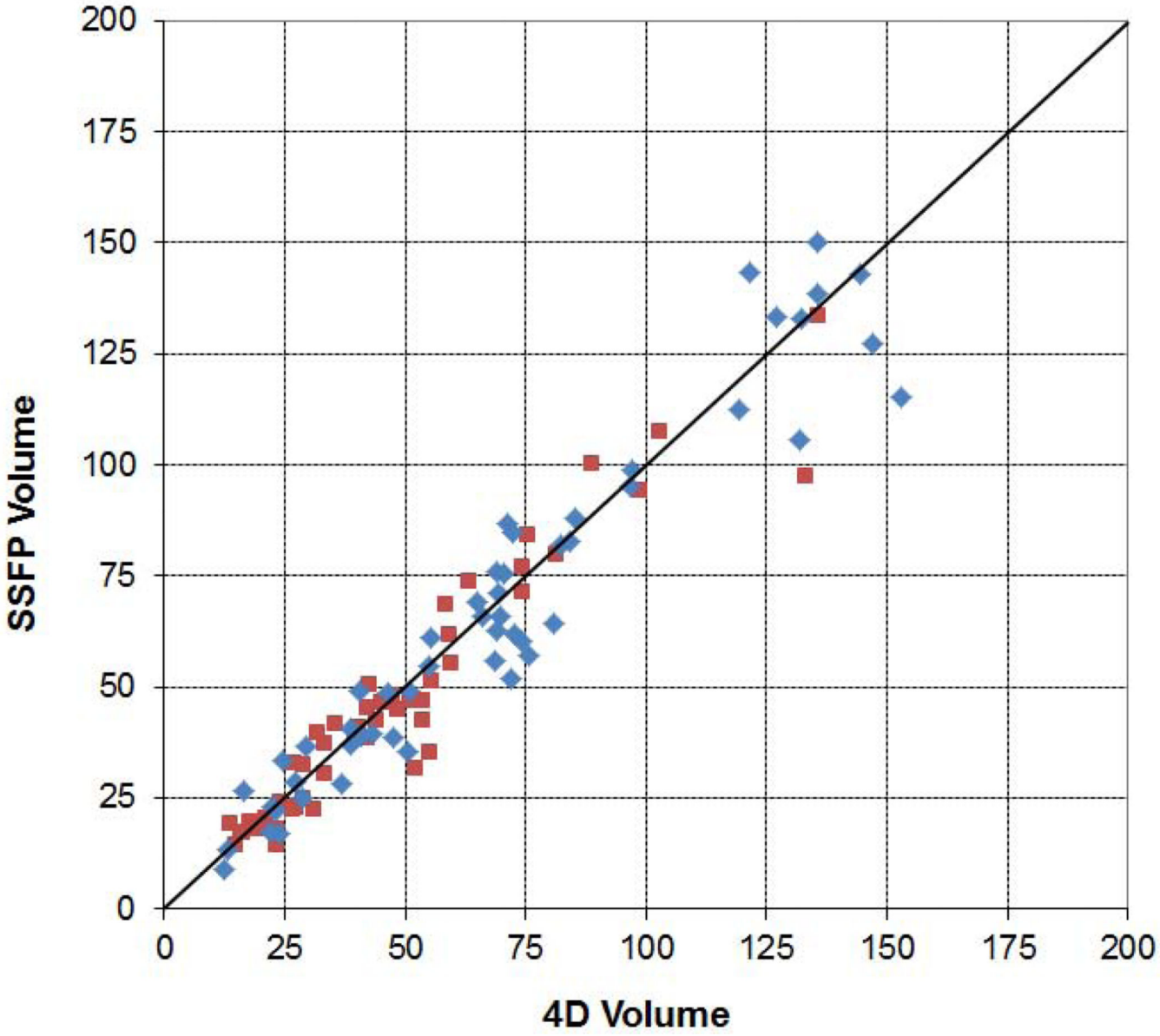

Figure 5.

Comparison of 4D-PC to conventional planar phase-contrast and SSFP volumetry. Net blood flow at the aortic and pulmonary valves (left) and regurgitant fractions at the aortic and pulmonary valves (middle) both show high correlation between 4D-PC and 2D-PC. Aortic measurements are shown in red squares, pulmonary measurements in blue diamonds. Volume measurements of the ventricles also show high correlation between 4D-PC and conventional MRI (right).

Table 1

Demographics and characteristics of patients included in the study.

Diagnosis / Indication	Age	Sex	BSA	Qp/Qs	AV RF	MV RF	PV RF	TV RF	GA
Pulmonary hypertension	7 yr	F	0.90	1.00	0	0	0	0	yes
Heart, liver transplant	8 yr	M	1.04	0.87	2	0	2	8	no
Query pulmonary sling	3 yr	M	0.63	0.87	0	1	2	5	yes
Total anomolous pulmonary venous return, post-repair	15 yr	M	0.71	0.99	0	4	1	8	no
Tetralogy of Fallot post-repair	6 yr	M	1.12	0.97	2	7	1	7	yes
Aortic coarctation, post-repair	6 yr	M	0.97	1.07	0	1	1	8	yes
Aortic coarctation, post-repair	12 yr	M	1.37	1.03	0	0	0	0	no
Interrupted aortic arch, post-repair	16 mo	M	0.42	1.12	1	0	0	2	yes
Aortic coarctation	4 yr	F	0.68	1.00	1	1	1	5	yes
Tetralogy of Fallot post-repair	15 yr	F	1.51	1.04	0	3	1	7	no
Atrial isomerism	5 yr	F	0.84	0.95	0	0	1	1	yes
Atrioventricular septal defect	6 yr	M	0.89	0.95	2	6	4	6	yes
Truncus arteriosus, post repair	7 yr	M	0.96	0.97	37	10	1	6	no
Aortic coarctation and insufficiency	10 mo	M	0.43	1.03	23	1	1	1	yes
Russell-Silver syndrome, Tetralogy of Fallot, AV repair	4 yr	F	0.50	0.87	9	10	0	3	yes
Tetralogy of Fallot post-repair	3 yr	M	0.63	1.03	0	0	46	0	yes
Tetralogy of Fallot post-repair	8 yr	F	0.73	0.85	2	2	61	0	yes
Pulmonary atresia, VSD post-repair	6 yr	F	0.64	1.09	0	2	41	6	yes
Tetralogy of Fallot post-repair	7 yr	F	0.91	1.02	5	3	35	3	yes
Tetralogy of Fallot post-repair	3 yr	M	0.53	0.96	1	7	15	24	yes
Ebstein anomaly	4 yr	F	0.69	0.90	0	1	19	15	yes
D-transposition of the great arteries, post-repair	6 yr	M	0.75	0.91	2	4	26	10	yes
Double-chamber right ventricle	6 yr	M	0.79	0.87	0	2	25	1	yes
Tetralogy of Fallot post-repair	3 yr	M	0.64	1.09	1	0	30	3	yes
Hemitruncus, interrupted aortic arch, post-repair	14 yr	M	1.68	0.99	0	2	0	20	no
Right pulmonary artery atresia	3 yr	F	0.63	1.00	0	5	0	12	yes
Atrial septal defect	13 yr	F	1.48	2.82	0	4	0	3	no

J Magn Reson Imaging. Author manuscript; available in PMC 2016 February 01.

Diagnosis / Indication	Age	Sex	BSA	Qp/Qs	AV RF	MV RF	PV RF	TV RF	GA
Tetralogy of Fallot post-repair, VSD patch leak	10 yr	F	1.01	0.87	0	0	6	10	yes
Right pulmonary artery atresia	2 yr	F	0.53	0.70	0	5	0	16	yes
Partial anomalous pulmonary venous return	6 yr	M	0.80	2.58	0	0	0	1	yes
ASD, cor triatriatum	7 yr	F	0.91	1.45	0	0	1	0	yes
DiGeorge syndrome, Tetralogy of Fallot post-repair	2 yr	F	0.46	0.52	0	3	31	2	yes
Critical pulmonary stenosis, bidirectional Glenn	11 yr	M	1.86	0.74	0	3	37	12	yes
Double outlet right ventricle, pulmonary artery aneurysm	8 yr	M	0.84	0.79	1	1	40	5	yes

BSA=body surface area, Dubois-Dubois, Qp/Qs=shunt fraction, AV=aortic valve, MV=mitral valve, PV=pulmonary valve, TV=tricuspid valve, RF=regurgitant fraction, GA=general anesthesia

Table 2

Comparison of net flow rates at each valve measured solely from 4D-PC anatomic and velocity field data with valve tracking at the inlet valves. Aortic and pulmonary valve measurements are most strongly correlated with the narrowest limits of agreement. There was slight underestimation of blood flow at the mitral and tricuspid valves relative to measurements at the outlet valves.

	AV vs PV	AV vs MV	AV vs TV	PV vs MV	PV vs TV	MV vs TV
Pearson correlation	0.988	0.967	0.963	0.940	0.955	0.940
B-A mean difference (L/min)	0.050	0.184	0.141	0.134	0.091	−0.042
B-A 95% limits of agreement (L/min)	0.411	0.658	0.715	0.822	0.754	0.746
B-A mean difference	2%	6%	5%	5%	3%	0%
B-A 95% limits of agreement	18%	26%	28%	34%	32%	25%

Table 3

Comparison of displaced ventricular volume and blood flow measured from 4D-PC before and after accounting for regurgitant blood flow at both the inlet and outlet valves. The strength of correlation and agreement between the two methodologies improves substantially after including the amount of regurgitant blood flow.

	LV vs AV	LV vs AV+AR+MR	RV vs PV	RV vs PV+PR+TR
Pearson correlation	0.854	0.939	0.813	0.948
B-A Mean difference (L/min)	0.31	0.11	0.67	0.08
B-A Limits of agreement (1.96 SD L/min)	1.34	0.88	1.45	0.79
B-A Mean difference	11%	4%	24%	3%
B-A Limits of agreement (1.96 SD)	43%	29%	54%	23%

Table 4

Comparison of net flow and regurgitant fraction measured by 4D-PC and conventional 2D phase-contrast MRI.

	AV net	AV RF	PV net	PV RF
Pearson correlation	0.935	0.972	0.934	0.933
B-A mean difference (L/min)	0.048	-	0.019	-
B-A 95% limits of agreement (L/min)	0.839	-	2.670	-
B-A mean difference	17%	2%	14%	1%
B-A 95% limits of agreement	29%	13%	38%	14%